Journal of Cellular Biochemistry 104:525–535 (2008)

Doxycycline Treatment Prevents Alveolar Destruction in VEGF-Deficient Mouse Lung

Harry B. Rossiter,[1] Miriam Scadeng,[2] Kechun Tang,[3] Peter D. Wagner,[3] and Ellen C. Breen[3]*

[1]Institute of Membrane and Systems Biology, University of Leeds, Leeds LS2 9JT, UK
[2]Center for Functional Magnetic Resonance Imaging, Department of Radiology, University of California, San Diego, La Jolla, California 92093-0623
[3]Division of Physiology, Department of Medicine, University of California, San Diego, La Jolla, California 92093-0623

Abstract In vivo lung-targeted VEGF gene inactivation results in pulmonary cell apoptosis, airspace enlargement, and increased lung compliance consistent with an emphysema-like phenotype. The predominant hypothesis for the cause of lung destruction in emphysema is an imbalance between active lung protease and anti-protease molecules. Therefore, we investigated the role of protease (e.g., matrix metalloproteinases—MMPs) and anti-protease (e.g., tissue inhibitors of metalloproteinases—TIMPs) expression in contributing to the lung structural remodeling observed in pulmonary-VEGF-deficient mice. VEGF*LoxP* mice instilled through the trachea with an adeno-associated virus expressing Cre recombinase (AAV/Cre) manifest airspace enlargement and a greater ($P < 0.05$) mean linear intercept (MLI: 44.2 ± 4.2 μm) compared to mice instilled with a control virus expressing LacZ (31.3 ± 2.5 μm). Airspace enlargement was prevented by the continuous administration of the general MMP inhibitor, doxycycline (Dox) (Cre + Dox: 32.6 ± 2.5 μm), and MLI values were not different from either control (LacZ + Dox: 30.5 ± 1.2 μm). In situ magnetic resonance imaging of VEGF gene inactivated mouse lungs revealed uneven inflation, residual trapped gas volumes upon oxygen absorption deflation/re-inflation, and loss of parenchymal structure; effects that were largely prevented by Dox. Five weeks after AAV/Cre infection Western blot revealed a 9.9-fold increase in pulmonary MMP-3, and 2-fold increases in MMP-9 and TIMP-2. However, the increase in MMP-3 was prevented by Dox administration and was associated with a 2-fold increase in serpin b5 (Maspin) expression. These results suggest that doxycycline treatment largely prevents the aberrant lung remodeling response observed in VEGF-deficient mouse lungs and is associated with changes in protease and anti-protease expression. J. Cell. Biochem. 104: 525–535, 2008.

Key words: serpin b5; tissue inhibitor of metalloproteinase; magnetic resonance imaging; extracellular matrix; Cre recombinase

Conditional lung-targeted VEGF gene inactivation through the pulmonary delivery of an adeno-associated virus (AAV) expressing Cre recombinase to adult VEGF*LoxP* mice has been demonstrated to result in an emphysema-like phenotype [Tang et al., 2004]. Lungs in these VEGF-deficient mice displayed increases in airspace size and a decrease in elastic recoil at both 5 and 8 weeks after virally mediated Cre delivery [Tang et al., 2004]. These observed structural changes, consistent with emphysema, persist despite a restoration of cellular VEGF levels by 8 weeks and suggest that permanent destructive remodeling has occurred in the lung during this period.

The predominant hypothesis for the cause of lung destruction in emphysema is an imbalance between active lung protease and anti-protease molecules [Wright and Churg, 2007]; a concept that has been supported from findings in several transgenic mouse models. For instance,

This article contains supplementary material, which may be viewed at the Journal of Cellular Biochemistry website at http://www.interscience.wiley.com/jpages/0730-2312/suppmat/index.html.

Grant sponsor: UC Tobacco-Related Disease Research Program; Grant number: 12Rt-0062; Grant sponsor: The Worldwide Universities Network, Research Mobility Programme.

*Correspondence to: Ellen C. Breen, Division of Physiology, Department of Medicine, 0623, UCSD, 9500 Gilman Drive, La Jolla, CA 92093-0623. E-mail: ebreen@ucsd.edu

Received 12 September 2007; Accepted 22 October 2007

DOI 10.1002/jcb.21643

over-expression of human MMP-1 in mice leads to pulmonary emphysema [D'Armiento et al., 1992], and gene deletion of macrophage elastase (MMP-12) or neutrophil elastase have both been shown to protect against cigarette smoke induced alveolar wall destruction [Hautamaki et al., 1997; Shapiro et al., 2003]. Furthermore, lung-targeted over-expression of inflammatory cytokines interferon-γ (IFN-γ) or IL-13 (each implicated in the progression of emphysema) have been reported to lead to emphysema-like structural changes in mouse lung and are accompanied by the increased expression of several MMPs and cathepsins [Wang et al., 2000; Zheng et al., 2000]. There is also increasing appreciation for the important role of lung protection and/or repair systems in defense of the elevated proteases and oxidant levels found in chronic obstructive pulmonary disease (COPD). Gene deletion of the anti-protease TIMP-3 or the host defense molecule Toll-like receptor 4 (TLR4) in mice have both been shown to result in the spontaneous development of emphysema characterized by increased gelatinase or elastinolytic activity [Leco et al., 2001; Zhang et al., 2006]. Similarly, inactivation of the alveolar epithelial cell expressed growth factor TGF-β1, through lung-targeted integrin αVβ6 gene deletion, has been shown to result in macrophage accumulation and MMP-12-dependent emphysema [Morris et al., 2003].

As such, and in view of the protective role of VEGF in cellular functions, we hypothesized that VEGF removal (via pulmonary Cre recombinase expression in VEGF*LoxP* mice) would result in an emphysema-like lung via an altered expression of protease and anti-protease genes. We therefore determined the expression of several MMPs and anti-proteases [serpin b5 (Maspin) and TIMPs 1–4] following lung-targeted VEGF gene ablation in adult mice. In addition, we hypothesized that the destructive elements of the structural remodeling observed in this model would be consequent to increased MMP expression and, therefore, that concurrent administration of the pan-MMP inhibitor doxycycline (Dox) would prevent alveolar destruction. Consequently, we evaluated the structural remodeling in Cre-expressing VEGF*LoxP* mice (and LacZ controls) with and without Dox administration using standard morphometric techniques [Tang et al., 2004] and in situ magnetic resonance imaging (MRI) [Scadeng et al., 2007].

METHODS

Materials

Doxycycline Hyclate (D-9891; Dox) was purchased from Sigma-Aldrich. Anti-MMP-2 (72 kDa Collagenase IV, Ab-7) was a rabbit polyclonal antibody (RB-1537-PO) from Neo-Markers (Fremont, CA). Anti-MMP-3 (AB-5; SL-IIIC4) and anti-MMP-7 (AB-4; PC492) were rabbit polyclonal antibodies from CalBiochem (La Jolla, CA). Anti-MMP-9 (RM105MMP9) was a rabbit polyclonal antibody to gelatinase B from Triple Point Biologics (Forest Grove, OR). MMP-12 (AB-2; IM1013) and TIMP-2 (AB-2; 67-4H11) antibodies were mouse monoclonal from CalBiochem. Rabbit polyclonal anti-Maspin (H-130, Serpin b5; sc-22762) and goat polyclonal anti-actin (1–19; SC-1616) were both from Santa Cruz Biotechnologies (Santa Cruz, CA). TIMP-3 (Loop-1; ab39184) was a rabbit polyclonal from AbCam, Inc.

VEGF*LoxP* Mice

The University of California, San Diego Animal Subjects Committee approved the reported study. Adult VEGF*LoxP* mice ($n = 96$ total) ranged in age from 2 to 5 months, and body mass averaged 23.9 ± 2.9 g at the beginning of the study. To site-specifically inactivate the pulmonary VEGF gene in adult mice, an adeno-associated virus expressing Cre recombinase (AAV/Cre), or a control virus (AAV/LacZ) ($n = 48$ in each viral group), was instilled through the trachea into the lungs of mice with *LoxP* sites flanking a portion of VEGF exon 3. VEGF*LoxP* mice were engineered by Ferrara and colleagues [Gerber et al., 1999] and previously used in our laboratory [Tang et al., 2004]. A VEGF*LoxP* mouse colony is maintained at the University of California, San Diego. Mice were kept on a 12:12-h day-night cycle and provided standard food and water. Half of the mice ($n = 24$ in each of the two viral groups) also received Dox, administered at 2 g/L in the drinking water starting on the same day as the viral delivery until euthanasia at either 5, 8, or 12 weeks. This resulted in four experimental groups ($n = 24$ in each) of virally infected and Dox-treated mice in a matrix design: LacZ; LacZ + Dox; Cre; and Cre + Dox.

AAV Production and Gene Delivery

An AAV helper-free system (Stratagene, La Jolla, CA [Xiao et al., 1998]) was used for the

production of recombinant AAV that expressed either Cre recombinase (AAV/Cre) or a control reporter gene, LacZ (AAV/LacZ). These recombinant viruses were generated using the complete reading frame of the Cre recombinase [Gu et al., 1994] or LacZ genes in addition to the HSV or cytomegalovirus (CMV) promoter and SV40 poly A sequence to create pAAV-Cre and pAAV-LacZ plasmids that carry the gene cassettes between two AAV2 long terminal repeats (LTRs). These constructs were then used to assemble recombinant AAVs in 293 packaging cells, as previously described [Tang et al., 2004]. AAVs were isolated by freeze-thawing and then purified over heparin-agarose columns (Sigma, HEP-1-5). For AAV delivery, VEGF*LoxP* mice were anesthetized with halothane and instilled through the trachea at a 45° angle (over ~1 min) with 100 μl of AAV/Cre or AAV/LacZ [1×10^{10} viral particles/mouse suspended in sterile phosphate-buffered saline (PBS)] and followed immediately by 200 μl perflubron (Rimar 101, Mitien, Trissino, Italy). Similar to previous studies [Tang et al., 2004] perflubron aided in viral delivery and distribution throughout the lung.

Mean Linear Intercept Estimates of Airspace Size

A point-count morphometric technique (mean linear intercept—MLI) was used to assess air space size according to the method of Thurlbeck [1967]. Eight weeks after infection, lungs from six mice in each of the four groups were degassed by ventilation with 100% O_2 for 10 min and fixed at an airway pressure of 20 cmH_2O with 4% paraformaldehyde before paraffin embedding. Multiple digital images from histological sections were systematically captured at 10× magnification. Images were overlaid with a 10×10 grid (1 mm^2), and MLI established from every second image (i.e., in a checkerboard fashion, averaging 11 images for each mouse). The distribution of the MLI values of all the digital photographs was assessed by frequency distribution analysis and characterized by use of a Gaussian model, as previously described [Tang et al., 2004].

In Situ Magnetic Resonance (MR) Lung Imaging

To visualize pulmonary structural changes in situ following the experimental treatments, six mice in each experimental group were prepared for MR imaging. Mice were anesthetized with pentobarbital (Nembutal™, 40–60 mg/kg, i.p.) 12 weeks post-infection, and the trachea cannulated with an 18GA, 1.1 mm × 48 mm Insyte™ i.v. plastic catheter (Becton Dickinson, NJ) and then ventilated with 100% O_2 for 10 min at an airway pressure of 10–12 cmH_2O. During ventilation, and 10 min before euthanasia, mice were injected with 0.4 ml (i.p.) of Gadolinium Dimeglumine (Magnevist®, Schering, Germany), heparin (500 units) and subsequently euthanized (pentobarbital 100–150 mg/kg body weight). After circulation had ceased mice were removed from the ventilator, placed at a 45° angle, and fluid instilled through the tracheal cannula. This was achieved by priming the cannula with approximately 100 μl of PBS (to remove any gas dead-space in the equipment), and then sequentially instilling with perfluoro-compound (PFC; FC-75®, Acros Organics, Belgium) to an airway pressure of 10 cmH_2O followed by PBS containing 0.05% (w/v) low melt agarose (NuSieve Agarose, Cambrex) to an airway pressure of 20 cmH_2O, as previously described [Scadeng et al., 2007]. Mice were imaged using a 5 cm custom built Quadrature volume MR imaging coil and a horizontal bore 7T MR scanner (GE, Milwaukee, OR). Images were acquired using a 2D spin echo sequence which resulted in an in-plane resolution of 112 μm and slice thickness of 300 μm. Images were evaluated (in a randomized sequence) for changes in pulmonary structure by a radiologist blinded to the experimental condition. Lungs that displayed no definitive structural alterations were classified as "normal." Lungs were classified as having an "emphysema-like structure" if the MR images revealed the presence of residual gas trapping, uneven mixing of the liquid contrast agents (PFC/PBS) and/or loss of parenchymal structural detail.

Real-Time RT-PCR Analysis

Five weeks post-viral-infection total mRNA levels of proteases (MMP-2, -3, -7, -9, -12, cathepsin K) and anti-proteases [TIMP-1, -2, -3, -4, α1-anti-trypsin (α1AT), and serpin b5 (Maspin)] were assessed using real-time RT-PCR. Cellular RNA was isolated from the lungs of six mice in each of the four experimental groups using TriPure Isolation Reagent (Roche Applied Science, Indianapolis, IN) and further purified using RNase-Free DNase I and RNeasy Mini columns (Qiagen, Valencia, CA). RNA was

quantitated by spectrophotometry and 450 ng of RNA was reverse transcribed using ThermoScript™ Reverse Transcriptase and an oligo (dT) primer (Invitrogen, Carlsbad, CA). Two microliters of the RT product was amplified using 2X SYBR® Green PCR Master Mix, 0.3 μM sense and anti-sense primers (see Table S1 in the Online Data Supplement) and 0.025 μM reference dye (ROX). PCR reactions were performed in an Mx3000P System (Stratagene) with an annealing temperature of 55°C for 40 cycles for all primers. An additional 30 min dissociation curve was run at the end of the amplification protocol to determine the specificity of the primers. No template and no RT controls were included to confirm RNA purity.

Western Blot Analysis

Five weeks post-infection, lung tissue from six mice in each of the four experimental groups was homogenized in 1% Triton X-100, 150 mM NaCl, 50 mM Tris, pH 7.5, Complete EDTA-free Protease Inhibitor Cocktail Tablet (Roche Diagnostics, Mannheim, Germany), 100 μl PMSF and quantitated using the Bio-RAD DC Protein assay. Protein samples (50 μg) were separated by 10% or 15% SDS–PAGE under reducing conditions (β-mercaptoethanol) using standard Laemmli sample buffer and Tris/Glycine/SDS running buffer. Protein samples were then elctrophoretically transferred to Immobilon P membrane in Transfer Buffer (20% methanol, 192 mM glycine, 25 mM Tris, pH 8, 0.001% SDS). Blots were blocked for 1 h in 5% milk, 0.02% Triton X-100, and anti-foam A and then incubated with primary antibodies overnight at 4°C. Primary antibody dilutions were 1:5,000 for MMP-7, MMP-9 and TIMP-3, 1:2000 for β-actin, 1:1000 for MMP-2, MMP-12 and serpin b5 (Maspin), 1:400 for MMP-3, and 1:200 for TIMP-2. Blots were washed and probed with HRP-conjugated secondary antibodies specific for rabbit (Amersham Biosciences, UK), goat (Southern Biotechnology Associates, Inc., Birmingham, AL) or mouse (DAKO Corporation, Denmark) and detected by chemiluminescence using the ECL™ Western Blotting Detection Reagents (Amersham Biosciences).

Statistical Analysis

Differences between the four experimental groups (2×2 matrix) were determined using a two-way ANOVA with significance at $P < 0.05$, and Scheffe's post hoc test where appropriate. The two factors considered were, (1) viral infection: Cre versus LacZ and, (2) protease inhibition treatment: Dox versus control. All values are reported as mean and standard deviation.

RESULTS

Eight weeks after pulmonary AAV infection, pulmonary airspace size was significantly increased in the AAV/Cre-infected (VEGF-deficient, and without Dox treatment) mouse lungs (Fig. 1). The MLI in Cre expressing mice averaged 44.2 ± 4.2 μm compared to 31.3 ± 2.5 μm in the LacZ group ($P < 0.05$). There was also a significant interaction between Cre expression and protease inhibition by Dox. Dox treatment prevented the MLI increase seen in the Cre group (Cre + Dox, 32.6 ± 2.5 μm), such that MLI in Cre + Dox was not different from either LacZ + Dox, (30.5 ± 1.2 μm) or from the untreated (LacZ only) controls. Furthermore, the heterogeneity of the MLI distribution (judged by the standard deviation [SD] of the Gaussian fit to the frequency analysis of the MLI values; Fig. 1) was increased in the Cre group (5.14 μm) compared to all other groups (LacZ, 2.96 μm; LacZ + Dox, 2.89 μm; Cre + Dox, 3.35 μm).

The MLI increase in the Cre group was consistent with the structural changes observed from in situ MR imaging (Fig. 2). Axial and coronal MR images allowed detailed observation of pulmonary airway and parenchymal structures. LacZ infected mice manifest ordered lung architecture (Fig. 2A,B) in which parenchymal structure and density was homogeneous and the high-contrast gadolinium-enhanced vascular structures were clearly delineated. An emphysema-like pulmonary structure was observed in Cre expressing (VEGF-deficient) mice (Fig. 2C,D). In these cases the lungs displayed distinct regions of residual or retained gas volume (contrast negative spots) and uneven distribution of the liquids instilled (PBS/PFC). These VEGF-gene ablated lungs also manifest a loss of structural detail throughout the parenchyma. For comparison, control lungs to which air was intentionally re-introduced during the liquid instillation procedure (positive control) are illustrated in Figure 2E,F. Results of a blinded analysis revealed that all of the LacZ lungs (six out of six mice) displayed no alterations in lung structure and were,

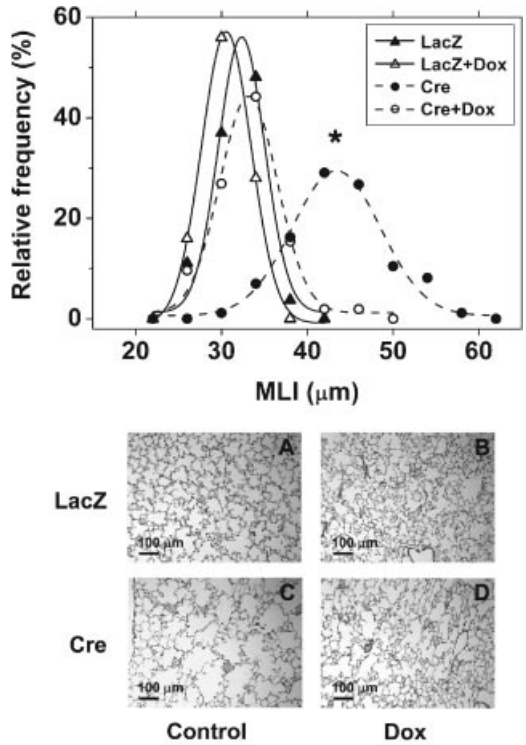

Fig. 1. Airspace enlargement in VEGF deficient lungs is prevented by MMP inhibition with doxycycline. (Top) The mean linear intercept (MLI) frequency distribution in VEGF*LoxP* transgenic mice infected with either AAV/Cre or AAV/LacZ in the presence and absence of doxycycline (Dox) at eight weeks post-infection. Values represent the distribution of chord lengths, n = 5–6 mice from each experimental group. *Represents significant difference ($P < 0.05$) from all other groups. (Bottom) Representative hematoxylin-stained lung sections from VEGF*LoxP* mouse lungs eight weeks post-infection with either: (**A**) AAV/LacZ; (**B**) AAV/LacZ + Dox; (**C**) AAV/Cre; or (**D**) AAV/Cre + Dox.

therefore, assigned as "normal" (Fig. 2A,B). 83% of Cre expressing lungs (five out of six mice) revealed emphysema-like structural changes (Fig. 2C,D). The addition of Dox did not allow clear differentiation between phenotypes (normal or emphysema-like) with four out of six mice in the LacZ + Dox group and three out of six mice in the Cre + Dox group manifesting a lung structure that was unaltered and assigned to the "normal" group (Fig. 2G,H).

MMP, TIMP and serpin b5 mRNA levels were measured by real-time RT-PCR (Fig. 3). Cre expression in VEGF*LoxP* mice increased MMP-3 mRNA levels ($P < 0.05$) 1.9-fold only in lungs of Dox treated mice. Cre expression in VEGF*LoxP* mice also increased MMP-9 mRNA levels by 3.7-fold compared to LacZ, but there was no effect of Dox treatment. Serpin b5 and TIMP-2 mRNA levels were increased ($P < 0.05$) 9.1- and 2.5-fold, respectively, in the Cre + Dox lungs compared to the LacZ + Dox control group. MMP-2, MMP-12, cathepsin K, TIMP-1, -3, and -4, and α1AT mRNA levels measured by real-time RT-PCR analysis were not different between each of the experimental groups (see Fig. S1 in the Online Data Supplement).

MMP, TIMP, and serpin b5 protein levels were measured by Western analyses (Fig. 4). Western blot detection of the active form of MMP-3 (45 kDa) revealed a 9.9-fold increase in MMP-3 levels in Cre expressing lungs compared to LacZ ($P < 0.05$). This increase in MMP-3 was prevented by Dox treatment: MMP-3 levels in Cre + Dox were not different from either of the LacZ groups ($P > 0.05$). MMP-9 and TIMP-2 expression were both increased ($P < 0.05$) by ~2-fold in Cre expressing lungs compared to LacZ, but showed no change with Dox treatment. Serpin b5 protein levels were significantly increased ($P < 0.05$) in the Cre + Dox group (~2-fold) compared to all other groups. MMP-2, -7, and -12 and TIMP-3 protein levels were unchanged between each of the groups (see Fig. S2 in the Online Data Supplement).

DISCUSSION

The lung is a highly vascularized organ in which VEGF is abundantly expressed by bronchial and alveolar epithelial cells and to a lesser extent by smooth muscle cells, fibroblasts, and macrophages [Fehrenbach et al., 1999]. In patients with severe emphysema, VEGF levels have been shown to be reduced in the bronchoalveolar lavage, sputum, and lung tissue [Kasahara et al., 2001; Koyama et al., 2002]. Using an adeno-associated viral vector (AAV) to deliver Cre recombinase to the airways of adult mice, we have previously observed that lung-targeted VEGF gene deletion leads to apoptosis and long-term emphysema-like changes in lung structure without an apparent inflammatory cell influx [Tang et al., 2004]. Therefore, we hypothesized that proteases expressed by alveolar epithelial and/or mesenchymal cells may contribute to the alveolar wall destruction observed in VEGF-deficient mouse lungs. The present study showed this to be the case, demonstrating that lung-targeted VEGF inactivation was accompanied by an increased expression of protease (specifically, MMP-3 and MMP-9) molecules. This was accompanied by

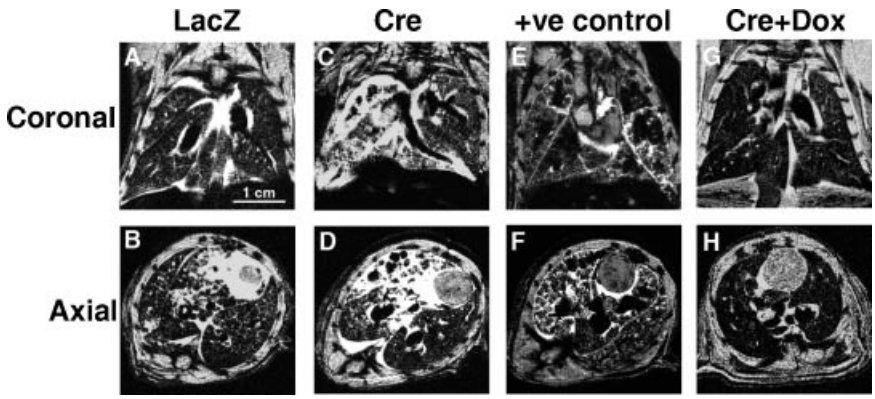

Fig. 2. Emphysema-like lung structure in Cre recombinase expressing VEGF*LoxP* mouse lungs imaged in situ by magnetic resonance. PFC/saline-filled lungs were imaged with a 7T magnet and 2D spin echo sequence resulting in a pixel resolution of 112 μm. Coronal (**A**,**C**,**E**,**G**) and axial (**B**,**D**,**F**,**H**) orientations are shown for LacZ, Cre and Cre + Dox experimental groups of mouse lungs at 12 weeks post-infection with recombinant AAVs (pulmonary structures in the LacZ + Dox group mirrored the LacZ group). Images A and B show LacZ lungs with normal lung structure. Images C and D illustrate a Cre expressing VEGF-deficient lung revealing an emphysema-like phenotype with regions of residual or retained gas volume (contrast negative spots), uneven distribution of the liquid instilled PBS/PFC, and loss of structural detail throughout the parenchyma. Images E and F show a positive control (LacZ) mouse lung where air was deliberately re-introduced during the fluid-instillation procedure ion order to illustrate the effect of ''trapped gas'' on the MR image—note the similarity between the appearance of ''trapped gas'' in the upper lobes of image E (positive control) and image C (Cre) and in the left lobes in images F (positive control) and D (Cre). This demonstrates that gas bubbles appear as dark contrast negative spots and contribute to degradation of overall image quality. Cre expressing VEGF*LoxP* mouse lungs were protected against structural remodeling following Dox administration (Cre + Dox), as shown in images G and H (i.e., similar to the LacZ controls; images A and B).

only a modest increase in expression of the anti-protease, TIMP-2. However, simultaneous VEGF-gene inactivation and treatment with a general MMP inhibitor (Dox) blocked the enhanced expression of MMP-3 and increased the expression of the anti-protease serpin b5 (Maspin). MMP inhibition by Dox also prevented alveolar wall destruction (assessed by the MLI estimate of airspace size), and reduced the incidence of lung structural alterations and retained gas trapping assessed in situ by MRI.

MMPs and the Regulation of Lung Injury and Repair

When the lung is exposed to injurious agents such as cigarette smoke or oxidants one of the first lines of defense is the epithelial cell layer. Increased epithelial cell turnover due

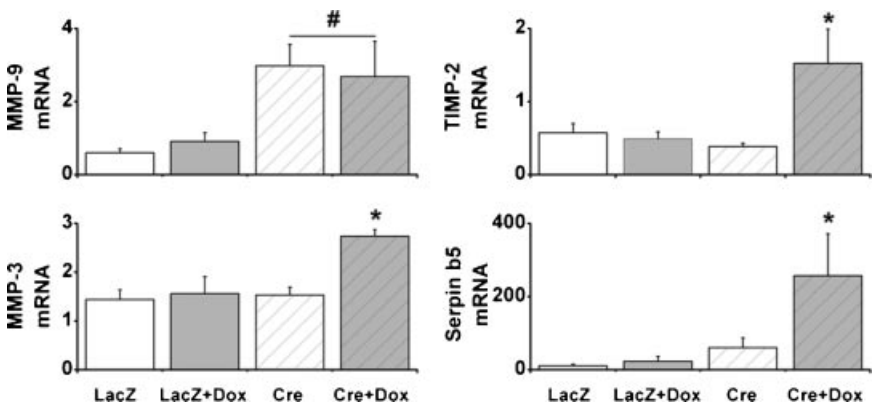

Fig. 3. Protease/anti-protease mRNA levels. Matrix metalloproteinases (MMPs) MMP-3, MMP-9 and anti-proteases TIMP-2 and serpin b5 (Maspin) mRNA levels measured by real-time RT-PCR analysis in VEGF*LoxP* mouse lungs 5 weeks after infection with either AAV/LacZ or AAV/Cre in the presence and absence of doxycycline (Dox). Relative mRNA levels (arbitrary units) were normalized to GAPDH mRNA. Values represent the mean (±SD), n = 4–6 per group. *Represents significant difference ($P < 0.05$) from all other groups; # represents significant difference ($P < 0.05$) between Cre and LacZ groups (with no interaction of Dox administration).

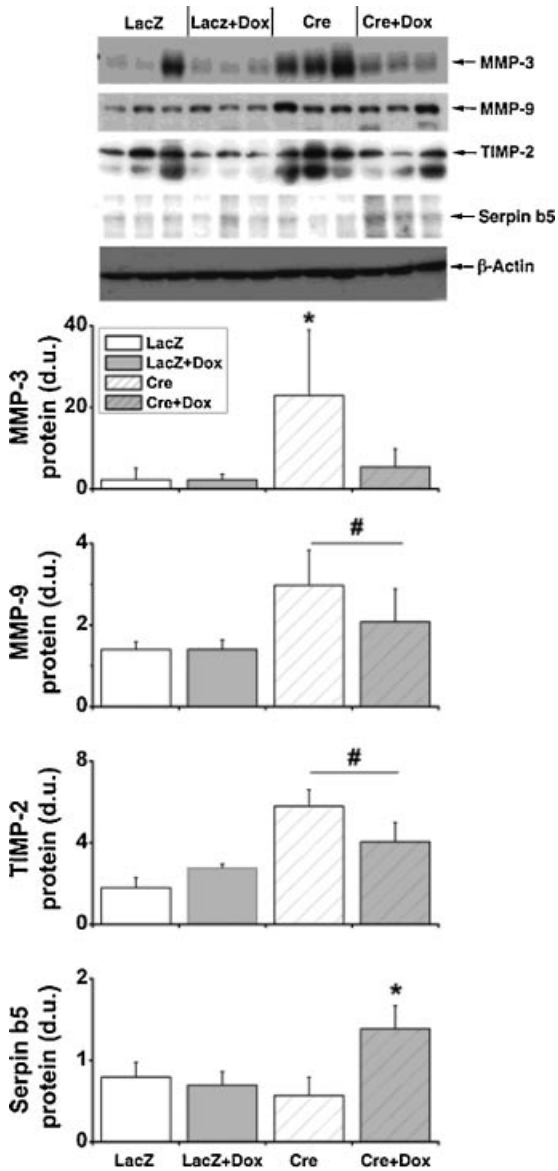

Fig. 4. Balance of proteases/anti-proteases in control and VEGF-deficient mouse lungs, with and without MMP inhibition by doxycycline (Dox). Representative Western blots of MMP-3, MMP-9, TIMP-2 and serpin b5 (Maspin) protein levels in VEGF-deficient lungs with and without MMP inhibition by Dox. Analysis was made in VEGF*LoxP* mouse lungs 5 weeks after infection with either AAV/LacZ or AAV/Cre. Each lane represents lung protein isolated from an individual mouse. Densitometry values represent the mean (±SD), n = 5–6 mouse lungs per group. *Represents significant difference ($P < 0.05$) from all other groups; # represents significant difference ($P < 0.05$) between Cre and LacZ groups (with no interaction of Dox administration).

to apoptosis initiates a repair process that, if successful, will repair the epithelium without altering the composition and organization of the underlying matrix. In the present study VEGF gene deletion and alveolar wall destruction was accompanied by enhanced expression of MMP-3 and -9. Like all MMPs, MMP-3 and -9 demonstrate substrate specificity in vitro for ECM proteins, including components of the alveolar–capillary barrier (collagens I, III, and IV, lamanin, and elastin [Sternlicht and Werb, 2001]), and could, therefore, directly contribute to alveolar destruction. In addition, several growth factor complexes (including TGF-β, CTGF, and VEGF) act as substrates for MMP-3 and MMP-9 [Bergers et al., 2000]. Lee et al. [2005] recently demonstrated that VEGF itself maybe intra-molecularly processed by MMP-3 into distinct biological isoforms that either promote the formation of large, dilated vessels or new capillary structures. Alternatively, MMP-3 expression could represent a cell population actively undergoing apoptosis as nuclear localized, active, MMP-3 has recently found to be a critical step in hepatic cancer cells undergoing apoptosis [Si-Tayeb et al., 2006]. Thus, it seems likely that MMP-3 and MMP-9 are integrally involved in the progression of the VEGF-dependent apoptosis and alveolar remodeling seen in the present study; whether this involvement is via a direct or indirect mechanism, however, remains to be resolved.

The Potential of Pulmonary Anti-Proteases to Limit Lung Destruction

In a normal repair process anti-proteases are thought to prevent excessive MMP activation and aberrant ECM remodeling [Gueders et al., 2006]. Four tissue inhibitors of metalloproteinases have been identified (TIMPs 1–4) in the lung [Selman et al., 2000]. The present study did not reveal significant differences in TIMP-1, -3, and -4 mRNA levels between the experimental groups. Only a modest increase in TIMP-2 mRNA was observed in the Dox-treated VEGF-deficient mouse lungs (Cre + Dox). Furthermore, Western analyses of TIMP-2 and -3 protein levels revealed only a small ~2-fold increase in TIMP-2 (normally expressed by parenchymal fibroblasts and epithelial cells [Selman et al., 2000]) and no change in TIMP-3 (normally expressed by type I cells) in AAV/Cre infected lungs.

However, the anti-protease serpin b5 was considerably (~9-fold) up-regulated in the Dox treated VEGF-inactivated mice in the present study. This serpin is a member of the mammary serine protease inhibitors (Maspin) family and was first identified as a tumor-suppressor gene

in human mammary epithelial cells [Zou et al., 1994]. Serpin b5 has been demonstrated to inhibit (in part) angiogenesis through its interaction with collagen types I and III [Zhang et al., 2000], and has additionally been shown to inhibit tumor growth and metastasis through a pro-apoptotic mechanism [Latha et al., 2005].

The best-known example of a serpin-family gene implicated in lung protection is that of α1 anti-trypsin (α1AT) deficiency which is found in approximately 1–3% of the patients diagnosed with COPD [Strange et al., 2006]. α1AT inhibits neutrophil elastase, and its over-expression has been shown to reduce airspace enlargement in cigarette smoke exposed mice [Churg et al., 2003]. Furthermore, α1AT over-expression in VEGF receptor inhibited (SU5416-treated) mice also decreased the incidence caspase 3-induced apoptosis and oxidative stress [Petrache et al., 2006]. Another serpin, Serpine-2, was recently reported to exhibit gene polymorphism in COPD patients [Demeo et al., 2006]. Therefore, while the role the anti-protease activity of serpin b5 in the lung is not as well established as that of the TIMPs or α1 anti-trypsin, both of these anti-protease families clearly have a role in regulating apoptosis, cell proliferation, and angiogenesis [Gill et al., 2006; Gueders et al., 2006].

Doxycycline and the Prevention of Emphysema

In the present study we used the potent MMP inhibitory activity of doxycycline as a tool for assessing the contribution of MMPs to the alveolar destruction observed in our pulmonary-targeted VEGF-deficient model of emphysema in mice. Doxycycline is a tetracycline derivative that was first found to inhibit collagenolytic activity in a study of diabetic-associated gingivitis via a mechanism independent of its anti-microbial properties [Golub et al., 1998]. At present doxycycline is the only clinically approved MMP inhibitor (Periostat) and is designated for the treatment of periodontal disease [Peterson, 2004]. However, in several patients and animal studies of diseases characterized by excessive extracellular matrix turnover (including cancer metastasis, aortic aneurysms, atherosclerotic plaques, myocardial infarction, and glomerulonephritis) Dox treatment has been found to improve disease symptoms [Golub et al., 1998; Ahuja, 2003; Garcia et al., 2007; Naini et al., 2007]. In the lung Dox administration has been found to inhibit MMP expression and activity, in particular MMP-2 and MMP-9, associated with asthma [Lee et al., 2004], lymphangioleiomyomatosis [Moses et al., 2006], LPS-induced injury [Fujita et al., 2007] and bleomycin-induced fibrosis [Fujita et al., 2006]. Dox has the ability to inhibit several MMPs, including those with specificity for fibrillar collagens, collagens (MMP-1, MMP-2, MMP-7, and MMP-13) as well as basement membrane, type IV collagen (MMP-2 and MMP-9) through both direct and indirect mechanisms [Golub et al., 1998]. Directly, Dox binds to specific MMP peptide regions and prevents enzyme activity through the chelation of calcium and/or zinc cations and alterations in tertiary enzyme structure. Indirectly, Dox can inhibit oxidative activation of the pro-MMP form into the active moiety. In addition to MMP inhibition, tetracycline derivatives may also inhibit serine proteases either directly [Imamura et al., 2001] or by protecting serine protease inhibitors, such as α1AT, from MMP-dependent degradation [Sorsa et al., 1993].

While Dox has many potential mechanisms by which it may limit or prevent alveolar remodeling in chronic pulmonary diseases, it has been suggested to predominantly act through the inhibition of MMP-9 expression and activity [Hosford et al., 2004]. In the present study, however, MMP-9 expression does not seem to have played a major role in the Cre-induced pulmonary remodeling response, whereas MMP-3 was increased approximately 10-fold in the gene-ablated condition. This large increase in MMP-3 was prevented by Dox treatment and was accompanied by a coordinated increase in the serine protease inhibitor, serpin b5 (maspin). The attenuation of MMP-3 protein expression in the Cre + Dox group was also associated with a modest, 2-fold, increase in MMP-3 mRNA expression, suggestive of a feedback mechanism to maintain active MMP-3 levels. Whether this is the case, however, cannot be determined from the present data. While these data are not conclusive, therefore, they are at least consistent with the suggestion that pulmonary structural remodeling in VEGF-gene ablated mouse lungs is manifest via an MMP-dependent pathway.

Another possibility is that Dox administration may protect the alveolar–capillary barrier

by regulating apoptosis. Evidence to support an anti-apoptotic role for Dox (in addition to protecting α1AT and possibly serpin b5, both of which have apoptotic regulatory roles) may involve the ability to inhibit plasmin activity. This more recently ascribed role for Dox was identified in an ischemia-reperfusion model of myocardial infarction [Griffin et al., 2005]. In that study Dox was proposed to inhibit plasmin activity and prevent myocyte detachment from the underlying matrix thereby attenuating subsequent apoptosis; all independent of MMP activity [Griffin et al., 2005; Franco et al., 2006]. Further support for Dox as an anti-apoptotic agent has been suggested from the study of neonatal ischemia reperfusion where Dox was shown provide neuroprotection through the prevention of caspase 3 [Jantzie et al., 2005]. Thus, the precise mechanism by which Dox prevents aberrant alveolar remodeling in our model of lung-targeted VEGF gene deletion will require further investigation into the several and varied potential mechanisms that could provide protection to the alveolar capillary barrier.

Lung Evaluation by MRI

In this study we characterized the architecture of VEGF-deficient lungs using both a standard point-count morphometric technique and a novel MR imaging technique that allows in situ characterization of pulmonary structures in the entire chest. This MR imaging technique illustrated, for the first time, the pattern of VEGF-gene ablation induced emphysema in mouse lungs showing significant areas of lung damage and trapped-gas typically in distal or apical regions. Furthermore, the uneven mixing of the two liquid contrast media (PFC and PBS) used to highlight lung structure during MR imaging reflected an inefficiency of Cre-expressing lungs to uniformly deflate during oxygen ventilation (oxygen absorption atelectasis) and subsequently re-inflate with an even distribution pattern. We therefore devised criteria for assigning each lung as "emphysema-like" from the MR images that were based on these structural and functional details. These criteria were: presence of residual gas volumes (or air trapping), loss of parenchymal details due to magnetic susceptibility at gas–tissue interfaces, and poor mixing of liquid installation media. Each of these criteria would not be likely to be delineated using light microscopy of fixed sections. While qualitative, this MR imaging technique proved to be very sensitive to structural and functional alterations, with six out of six LacZ control mice being assigned to the "normal" phenotype and five out of six Cre-expressing assigned to the "emphysema-like" phenotype by a radiologist blinded to the experimental conditions. In addition, this MR-based technique appeared to be very sensitive to detection of even small amounts residual gas volume, because even small areas of air–tissue interface generate relative large MR susceptibility artifacts. It is perhaps particularly meaningful, therefore, that 50% of the Cre + Dox mice appeared "normal," suggesting that the degree of protection in these three Cre + Dox mice may have been essentially complete: a feature that was supported by the findings from the MLI (Fig. 1).

Summary

Lung-targeted VEGF gene deletion led to an emphysema-like phenotype with airspace enlargement, as well as evidence of loss of lung structure and gas trapping. This emphysema-like phenotype was accompanied by increased levels of MMP-3, -9 and TIMP-2. Since the proteases MMP-3 and -9 both have the potential to activate growth factors, including VEGF [Bergers et al., 2000; Lee et al., 2005], the present study suggests that increased MMP-3 expression in VEGF-deficiency may reflect a feedback-loop to maintain bioactive VEGF levels. However, as MMP-3 also plays a key role in tissue destruction (with specificity for components of the alveolar–capillary barrier; collagen IV, lamanin, and elastin [Sternlicht and Werb, 2001]) and possibly the apoptotic process [Si-Tayeb et al., 2006]. Notably the present data show that VEGF-dependent MMP-3 expression was blocked by the pan-MMP inhibitor doxycycline, which also resulted in an increased expression of the anti-protease and apoptotic regulator, serpin b5. However, whether the aberrant lung remodeling in VEGF-deficient mouse lungs occurred through an MMP-3 initiated mechanism, or via other cellular events attenuated (or inhibited) by Dox treatment, remains to be determined. Similarly, the present study also implies a novel role for serpin b5 in VEGF-dependent pulmonary remodeling, however, the precise role of the anti-protease or anti-apoptotic activity of this and TIMPs 1–4 to

moderate this remodeling requires further investigation.

REFERENCES

Ahuja TS. 2003. Doxycycline decreases proteinuria in glomerulonephritis. Am J Kidney Dis 42:376–380.

Bergers G, Brekken R, McMahon G, Vu TH, Itoh T, Tamaki K, Tanzawa K, Thorpe P, Itohara S, Werb Z, Hanahan D. 2000. Matrix metalloproteinase-9 triggers the angiogenic switch during carcinogenesis. Nat Cell Biol 2:737–744.

Churg A, Wang RD, Xie C, Wright JL. 2003. alpha-1-Antitrypsin ameliorates cigarette smoke-induced emphysema in the mouse. Am J Respir Crit Care Med 168: 199–207.

D'Armiento J, Dalal SS, Okada Y, Berg RA, Chada K. 1992. Collagenase expression in the lungs of transgenic mice causes pulmonary emphysema. Cell 71:955–961.

Demeo DL, Mariani TJ, Lange C, Srisuma S, Litonjua AA, Celedon JC, Lake SL, Reilly JJ, Chapman HA, Mecham BH, Haley KJ, Sylvia JS, Sparrow D, Spira AE, Beane J, Pinto-Plata V, Speizer FE, Shapiro SD, Weiss ST, Silverman EK. 2006. The SERPINE2 gene is associated with chronic obstructive pulmonary disease. Am J Hum Genet 78:253–264.

Fehrenbach H, Kasper M, Haase M, Schuh D, Muller M. 1999. Differential immunolocalization of VEGF in rat and human adult lung, and in experimental rat lung fibrosis: Light, fluorescence, and electron microscopy. Anat Rec 254:61–73.

Franco C, Ho B, Mulholland D, Hou G, Islam M, Donaldson K, Bendeck MP. 2006. Doxycycline alters vascular smooth muscle cell adhesion, migration, and reorganization of fibrillar collagen matrices. Am J Pathol 168:1697–1709.

Fujita M, Ye Q, Ouchi H, Harada E, Inoshima I, Kuwano K, Nakanishi Y. 2006. Doxycycline attenuated pulmonary fibrosis induced by bleomycin in mice. Antimicrob Agents Chemother 50:739–743.

Fujita M, Harada E, Ikegame S, Ye Q, Ouchi H, Inoshima I, Nakanishi Y. 2007. Doxycycline attenuated lung injury by its biological effect apart from its antimicrobial function. Pulm Pharmacol Ther 20:669–675.

Garcia RA, Go KV, Villarreal FJ. 2007. Effects of timed administration of doxycycline or methylprednisolone on post-myocardial infarction inflammation and left ventricular remodeling in the rat heart. Mol Cell Biochem 300:159–169.

Gerber HP, Hillan KJ, Ryan AM, Kowalski J, Keller GA, Rangell L, Wright BD, Radtke F, Aguet M, Ferrara N. 1999. VEGF is required for growth and survival in neonatal mice. Development 126:1149–1159.

Gill SE, Pape MC, Leco KJ. 2006. Tissue inhibitor of metalloproteinases 3 regulates extracellular matrix–cell signaling during bronchiole branching morphogenesis. Dev Biol 298:540–554.

Golub LM, Lee HM, Ryan ME, Giannobile WV, Payne J, Sorsa T. 1998. Tetracyclines inhibit connective tissue breakdown by multiple non-antimicrobial mechanisms. Adv Dent Res 12:12–26.

Griffin MO, Jinno M, Miles LA, Villarreal FJ. 2005. Reduction of myocardial infarct size by doxycycline: A role for plasmin inhibition. Mol Cell Biochem 270:1–11.

Gu H, Marth JD, Orban PC, Mossmann H, Rajewsky K. 1994. Deletion of a DNA polymerase beta gene segment in T cells using cell type-specific gene targeting. Science 265:103–106.

Gueders MM, Foidart JM, Noel A, Cataldo DD. 2006. Matrix metalloproteinases (MMPs) and tissue inhibitors of MMPs in the respiratory tract: Potential implications in asthma and other lung diseases. Eur J Pharmacol 533:133–144.

Hautamaki RD, Kobayashi DK, Senior RM, Shapiro SD. 1997. Requirement for macrophage elastase for cigarette smoke-induced emphysema in mice. Science 277:2002–2004.

Hosford GE, Fang X, Olson DM. 2004. Hyperoxia decreases matrix metalloproteinase-9 and increases tissue inhibitor of matrix metalloproteinase-1 protein in the newborn rat lung: Association with arrested alveolarization. Pediatr Res 56:26–34.

Imamura T, Matsushita K, Travis J, Potempa J. 2001. Inhibition of trypsin-like cysteine proteinases (gingipains) from Porphyromonas gingivalis by tetracycline and its analogues. Antimicrob Agents Chemother 45: 2871–2876.

Jantzie LL, Cheung PY, Todd KG. 2005. Doxycycline reduces cleaved caspase-3 and microglial activation in an animal model of neonatal hypoxia-ischemia. J Cereb Blood Flow Metab 25:314–324.

Kasahara Y, Tuder RM, Cool CD, Lynch DA, Flores SC, Voelkel NF. 2001. Endothelial cell death and decreased expression of vascular endothelial growth factor and vascular endothelial growth factor receptor 2 in emphysema. Am J Respir Crit Care Med 163:737–744.

Koyama S, Sato E, Haniuda M, Numanami H, Nagai S, Izumi T. 2002. Decreased level of vascular endothelial growth factor in bronchoalveolar lavage fluid of normal smokers and patients with pulmonary fibrosis. Am J Respir Crit Care Med 166:382–385.

Latha K, Zhang W, Cella N, Shi HY, Zhang M. 2005. Maspin mediates increased tumor cell apoptosis upon induction of the mitochondrial permeability transition. Mol Cell Biol 25:1737–1748.

Leco KJ, Waterhouse P, Sanchez OH, Gowing KL, Poole AR, Wakeham A, Mak TW, Khokha R. 2001. Spontaneous air space enlargement in the lungs of mice lacking tissue inhibitor of metalloproteinases-3 (TIMP-3). J Clin Invest 108:817–829.

Lee KS, Jin SM, Kim SS, Lee YC. 2004. Doxycycline reduces airway inflammation and hyperresponsiveness in a murine model of toluene diisocyanate-induced asthma. J Allergy Clin Immunol 113:902–909.

Lee S, Jilani SM, Nikolova GV, Carpizo D, Iruela-Arispe ML. 2005. Processing of VEGF-A by matrix metalloproteinases regulates bioavailability and vascular patterning in tumors. J Cell Biol 169:681–691.

Morris DG, Huang X, Kaminski N, Wang Y, Shapiro SD, Dolganov G, Glick A, Sheppard D. 2003. Loss of integrin alpha(v)beta6-mediated TGF-beta activation causes MMP12-dependent emphysema. Nature 422:169–173.

Moses MA, Harper J, Folkman J. 2006. Doxycycline treatment for lymphangioleiomyomatosis with urinary monitoring for MMPs. N Engl J Med 354:2621–2622.

Naini AE, Harandi AA, Moghtaderi J, Bastani B, Amiran A. 2007. Doxycycline: A pilot study to reduce diabetic proteinuria. Am J Nephrol 27:269–273.

Peterson JT. 2004. Matrix metalloproteinase inhibitor development and the remodeling of drug discovery. Heart Fail Rev 9:63–79.

Petrache I, Fijalkowska I, Zhen L, Medler TR, Brown E, Cruz P, Choe KH, Taraseviciene-Stewart L, Scerbavicius R, Shapiro L, Zhang B, Song S, Hicklin D, Voelkel NF, Flotte T, Tuder RM. 2006. A novel anti-apoptotic role for alpha-1 antitrypsin in the prevention of pulmonary emphysema. Am J Respir Crit Care Med 173:1222–1228.

Scadeng M, Rossiter HB, Dubowitz DJ, Breen EC. 2007. High-resolution three-dimensional magnetic resonance imaging of mouse lung in situ. Invest Radiol 42: 50–57.

Selman M, Ruiz V, Cabrera S, Segura L, Ramirez R, Barrios R, Pardo A. 2000. TIMP-1, -2, -3, and -4 in idiopathic pulmonary fibrosis. A prevailing nondegradative lung microenvironment? Am J Physiol Lung Cell Mol Physiol 279:L562–L574.

Shapiro SD, Goldstein NM, Houghton AM, Kobayashi DK, Kelley D, Belaaouaj A. 2003. Neutrophil elastase contributes to cigarette smoke-induced emphysema in mice. Am J Pathol 163:2329–2335.

Si-Tayeb K, Monvoisin A, Mazzocco C, Lepreux S, Decossas M, Cubel G, Taras D, Blanc JF, Robinson DR, Rosenbaum J. 2006. Matrix metalloproteinase 3 is present in the cell nucleus and is involved in apoptosis. Am J Pathol 169:1390–1401.

Sorsa T, Lindy O, Konttinen YT, Suomalainen K, Ingman T, Saari H, Halinen S, Lee HM, Golub LM, Hall J, Simon S. 1993. Doxycycline in the protection of serum alpha-1-antitrypsin from human neutrophil collagenase and gelatinase. Antimicrob Agents Chemother 37:592–594.

Sternlicht MD, Werb Z. 2001. How matrix metalloproteinases regulate cell behavior. Annu Rev Cell Dev Biol 17:463–516.

Strange C, Stoller JK, Sandhaus RA, Dickson R, Turino G. 2006. Results of a survey of patients with alpha-1 antitrypsin deficiency. Respiration 73:185–190.

Tang K, Rossiter HB, Wagner PD, Breen EC. 2004. Lung-targeted VEGF inactivation leads to an emphysema phenotype in mice. J Appl Physiol 97:1559–1566.

Thurlbeck WM. 1967. Internal surface area and other measurements in emphysema. Thorax 22:483–496.

Wang Z, Zheng T, Zhu Z, Homer RJ, Riese RJ, Chapman HA, Jr., Shapiro SD, Elias JA. 2000. Interferon gamma induction of pulmonary emphysema in the adult murine lung. J Exp Med 192:1587–1600.

Wright JL, Churg A. 2007. Current concepts in mechanisms of emphysema. Toxicol Pathol 35:111–115.

Xiao X, Li J, Samulski RJ. 1998. Production of high-titer recombinant adeno-associated virus vectors in the absence of helper adenovirus. J Virol 72:2224–2232.

Zhang M, Volpert O, Shi YH, Bouck N. 2000. Maspin is an angiogenesis inhibitor. Nat Med 6:196–199.

Zhang X, Shan P, Jiang G, Cohn L, Lee PJ. 2006. Toll-like receptor 4 deficiency causes pulmonary emphysema. J Clin Invest 116:3050–3059.

Zheng T, Zhu Z, Wang Z, Homer RJ, Ma B, Riese RJ, Jr., Chapman HA, Jr., Shapiro SD, Elias JA. 2000. Inducible targeting of IL-13 to the adult lung causes matrix metalloproteinase- and cathepsin-dependent emphysema. J Clin Invest 106:1081–1093.

Zou Z, Anisowicz A, Hendrix MJ, Thor A, Neveu M, Sheng S, Rafidi K, Seftor E, Sager R. 1994. Maspin, a serpin with tumor-suppressing activity in human mammary epithelial cells. Science 263:526–529.